International Conference on Mechanical System Engineering and Technology Applications (ICoMSETA) 2024, pp. X – XX

Enhancing weld quality through TIG/MIG hybrid welding: A CFD approach on the investigation of current density distribution and heat flux

Aisyah Arina Mohammad Shahrazel[1*], Nor Zaiazmin Yahaya[2], Mohamad Shaiful Ashrul Ishak[3], Ahmad Nazri Dagang[4], Mohd Fadzil Abdul Kadir[5], Sarizam Mamat[6]

[1,2,3] Carbon Clean Research Group, Faculty of Mechanical Engineering & Technology, Universiti Malaysia Perlis, Pauh Putra Campus, 02600 Arau, Perlis, Malaysia
[4] Faculty of Ocean Engineering Technology and Informatics, Universiti Malaysia Terengganu, 21030 Kuala Nerus, Terengganu, Malaysia
[5] Faculty of Informatics and Computing, Universiti Sultan Zainal Abidin, Besut Campus, 22200 Besut, Terengganu, Malaysia
[6] Faculty of Engineering and Technoloy, Universiti Malaysia Kelantan, Jeli Campus, 17600 Jeli, Kelantan, Malaysia

[*]E-mail: s211052244@studentmail.unimap.edu.my

Abstract. This research paper presents a numerical modeling study on the arc interaction of the TIG/MIG hybrid welding process, with a focus on current density distribution and heat flux at the MIG and TIG tips. By changing the current and voltage during welding, the aim is to understand the phenomena that occur during the interaction of the arc and its influence on the welding results. The study uses a computational fluid dynamics (CFD) approach using the ANSYS software package for thermal-electric and Fluent analysis. The simulation investigated a hybrid TIG/MIG welding process with a constant shielding gas flow of 1.0 m/s. The current varied from 180 A to 220 A and the voltage from 24 V to 26 V. The results show that the current level affects the current density distribution, with higher currents leading to higher current densities near the TIG tip. The heat flux is found to be not influenced by both current and voltage. The simulation results demonstrate heat flux variation errors of 2.16% for the TIG tip and 4.96% for the MIG tip when compared to experimental values, confirming the model's accuracy. This research improves understanding of heat flux contribution in hybrid welding and provides important knowledge of arc interaction and its impact on welding results. The findings contribute to the advancement of TIG/MIG hybrid welding technology and lay the groundwork for further exploration in the arc welding additive manufacturing field.

Keywords: Aluminium alloys, Hybrid-welding, Mechanical Properties, CFD Analysis.

1. Introduction

Traditional experimental approaches to welding process optimization involve extensive testing, real-world testing, and costly material consumption [1]. However, technology is evolving and researchers are increasingly turning to digital modeling and simulation as an alternative route [2]. Today, optimization involves numerical simulation, which provides an alternative route to explain and understand complex welding processes [3]. With the involvement of computational models, people can replicate and analyze the complex interactions between temperature, shielding gas flow rate, arc length, and current density. According to Sangwan et al., the gas flow rate (GFR) and TIG current are identified as the most influential operational parameters [4]. Besides, voltage and current are critical parameters in welding that can affect the heat input and, consequently, the band gap. The electric arc is a plasma of ionized gas that conducts electric current, producing high temperatures that melt the base and filler metals. Both current and voltage are essential in the process of welding. The amount of weld metal deposited during welding is influenced by the welding current applied. It impacts the depth of penetration and the melt-off rate of the electrode into the base material. In the investigation conducted by Zong and his colleagues, the current-voltage waveform during welding was used to examine the arc stability. When the TIG arc leads, it was discovered that the hybrid arc is more stable than traditional MIG. Instead of using 50 A current, the TIG current should be greater than 100 A to avoid spattering when the TIG arc trails but in their case the material used is mild steel [5]. Voltage measures the pressure that allows electrons to flow in the electrical circuit. In welding, it affects the heat generated by the arc. The higher the voltage, the greater the heat input, influencing weld penetration and overall quality. Gou and Wang used the 5052 aluminium alloy in their study. They vary the parameter of TIG welding at 100-120 A current and the fusion zone and the heat affected zone (HAZ) become larger when setting the current in that particular range increasingly [6]. Cui et al. conducted a study to explore the hybridization of TIG and MIG arcs in welding. They found that thermal efficiency decreased by about 10% under hybrid conditions compared to using the TIG or MIG arc heat sources. In addition, the efficiency of the TIG power source during hybrid welding was found to be lower than that of single TIG welding [7]. Understanding these concepts is essential to optimizing welding processes and achieving the desired welding properties. This study uses a CFD approach to investigate current density distribution and heat flux to improve welding quality through TIG/MIG hybrid welding.

2. CFD Simulations

The study involves using ANSYS software for CFD simulations, specifically focusing on thermal electric and Fluent analysis. A 2D domain representing the welding setup has been created. The welding tips are modeled as circular, with a diameter of 3.2 mm for the TIG tip and 1.2 mm for the feeding wire at the MIG tip, as shown in Figure 1.

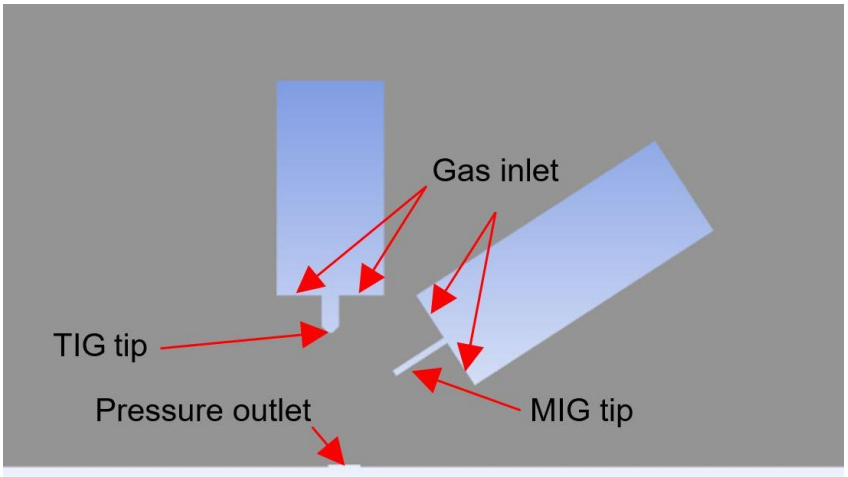

Figure 1. Two-dimensional domain

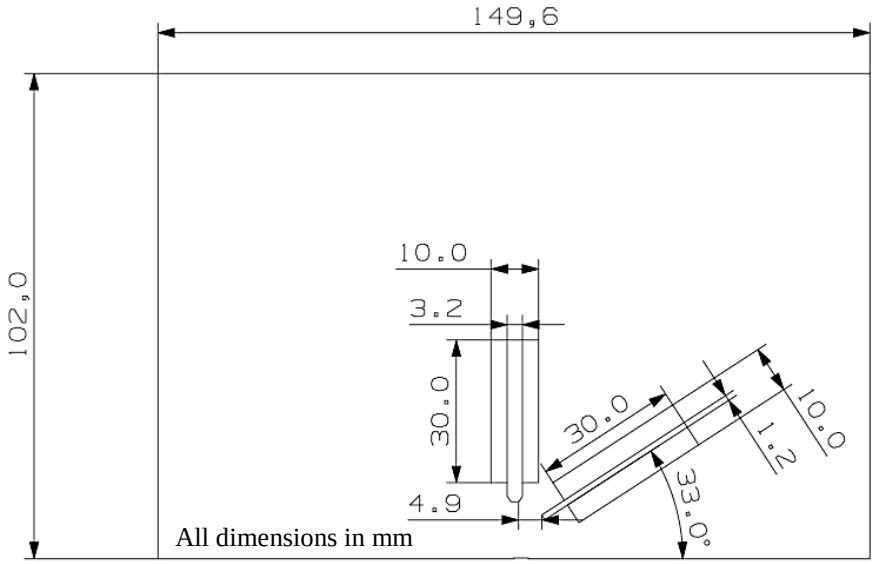

Figure 2. Two-dimensional domain dimension

Base metal is modeled together with an enclosed drawing of open-air 102 x 150 mm. The surface geometry is discretized into a computational mesh for numerical analysis as shown in Figure 3 and Figure 4 and the information is shown in Table 1. The meshing types and sizes were defined.

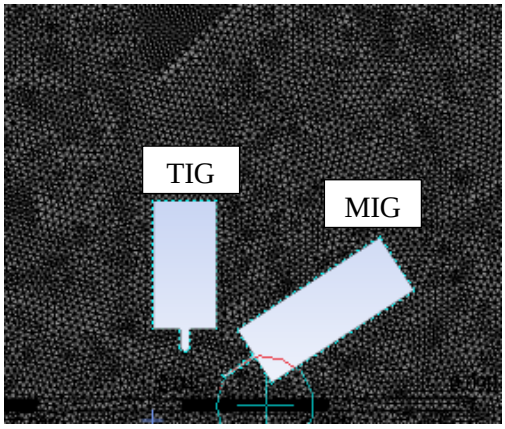

Figure 3. Thermal-electric mesh

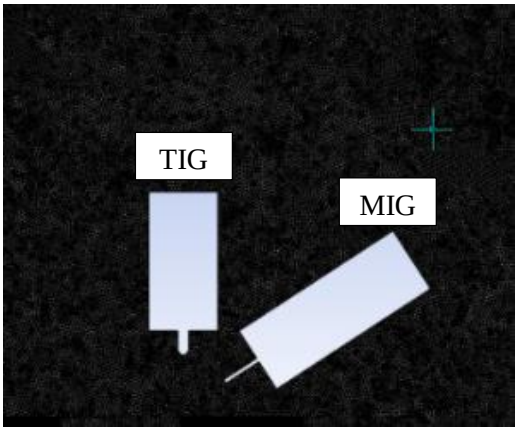

Figure 4. Fluent mesh

Table 1. Meshing information

Information	Thermal-Electric	Fluent
Max element	32 000	152 000
Mesh type	Triangles	Triangles
Mesh size	0.001 m	0.00047 m
Number of nodes	63 111	71 083
Number of elements	31 226	140 778
Skewness (average value)	0.051	-

Thermal-electric and Fluent analyses are performed to study arc behaviour. The simulation was performed for each set of current-voltage conditions and the resulting current density distribution and heat flux were recorded. Also the second simulation, the value of heat flux was used to run the Fluent analysis. One of the parameters from simulation results is compared with previous results to ensure accuracy. Equations (1) to (5) collectively describe the interaction of thermal and electromagnetic fields in a material while CFD used equations (6) to (12) for the numerical simulation of the welding process.

Heat Equation:

$$\rho C \frac{\partial T}{\partial t} + \nabla \cdot q = \dot{q} \tag{1}$$

Maxwell-Ampère Equation:

$$\nabla \cdot \left(J + \frac{\partial D}{\partial t} \right) = 0 \tag{2}$$

Fourier's Law of Heat Conduction:

$$q = (\Pi) \cdot y - \lambda \cdot \nabla T \tag{3}$$

Ohm's Law:

$$J = (\sigma) \cdot (E - \alpha \cdot \nabla T) \tag{4}$$

Constitutive Relation for Dielectric Materials:

$$D = (\varepsilon) \cdot \mathrm{E} \tag{5}$$

Mass continuity:

$$\frac{\partial \rho}{\partial t} + \nabla \cdot (\rho \vec{u}) = 0 \tag{6}$$

Momentum conservation:

$$\frac{\partial (\rho \vec{U})}{\partial t} + \nabla \cdot (\rho \vec{u} \otimes \vec{u}) = -\nabla p + \nabla \cdot \tau + \rho \vec{g} + \vec{j} \times \vec{B} + \vec{F}_{ST} + \vec{F}_{SLD} \tag{7}$$

Energy conservation:

$$\frac{\partial (\rho h)}{\partial t} + \nabla \cdot (p \vec{u} h) = \nabla \cdot (k \nabla T) + \frac{j^2}{\sigma} + Q_{rad} + S \tag{8}$$

Electric potential:

$$\nabla \cdot (\sigma \nabla \varphi) = 0 \tag{9}$$

Magnetic vector potential:

$$\nabla^2 \vec{A} = -\mu_0 \vec{j} \tag{10}$$

Ohm's Law:

$$\vec{J} = -\sigma \nabla \varphi \tag{11}$$

Magnetic field:

$$\vec{B} = \nabla \times \vec{A} \tag{12}$$

Table 2. Table of symbols

Symbol	Description	Symbol	Description
ρ	Density, kg/m³	p	Momentum per unit volume, kg/m^2.s
C	Specific heat capacity, J/(kg - K)	τ	Fluid pressure, Pa
T	Absolute temperature, K	J	Stress tensor, Pa
$\dot{q}$	Heat generation rate per unit volume, W/m³	B	Current density, A/m^2
Q	Heat flux vector, W/m²	F_{ST}	Magnetic field, T
J	Electric current density vector, A/m²	F_{SLD}	Surface tension force, N/m^3
E	Electric field intensity vector, V/m	h	Solid-liquid drag force, N/m^3
D	Electric flux density vector, C/m²	u	Specific enthalpy, J/kg
λ	Thermal conductivity matrix, W/m.K	k	Thermal conductivity, W/m.K
α	Seebeck coefficient matrix, V/K	σ	Electrical conductivity, S/m
Π	Peltier coefficient matrix, V	φ	Electric potential, V
ε	Dielectric permittivity matrix, F/m	μ_0	Permeability of free space, H/m
ρ	The fluid density, kg/m^3	A	Magnetic vector potential, T.m
u	Velocity, m/s	g	Acceleration due to gravity, m/s^2

3. Result and Discussion

Using the numerical simulation approach, the simulation approximation is the resulting outcome. The results of the simulation are presented in this section. Three set parameters have been determined as the features of the environment of the real welding process. Two module analyses have been done. Results in Table 3 and Table 4 show the current density and heat flux output at the TIG tip and MIG tip when varying the current and voltage when operating TIG/MIG hybrid welding on 6061 Aluminium Alloy.

3.1. Thermal-Electric analysis

Thermal-electric analysis reveals the distribution of current density and heat flux at the tips of MIG and TIG torches. Current and voltage are considered heat inputs for this hybrid welding process. For the current density distribution, the observation studies the current density distribution throughout the TIG/MIG hybrid welding process, focusing on the results of different current and voltage values. The red zones in these figures (Figures 5 to Figure 7) represent regions with the highest current density, particularly near the TIG tip. The greater current used during the welding process causes the high current density in these locations. To produce the extreme heat needed to melt the base and the charge components, this current concentration is essential. The most electrically active region, indicated by the red zone, indicates the strongest welding arc. This may have a direct impact on weld quality, as higher current density can be heated more intensely, affecting penetration depth and overall integrity. Giving deep penetration and strong fusion of materials can improve the efficiency of the welding process. With thinner materials, this very high current density can cause problems such as spatter or burning. Hence, the size and intensity of the red zone can be precisely controlled to maximize welding results by adjusting the current. However, in this study, the current density will not be included in the boundary condition in the next simulation, which is the Fluent analysis.

Table 3. Current density result

THERMAL- ELECTRIC	Set	Current and Voltage	Result
CURRENT DENSITY	1	TIG: 180 A, MIG: 24 V	Figure 5
	2	TIG: 200 A, MIG: 25 V	Figure 6
	3	TIG: 220A, MIG: 26 V	Figure 7

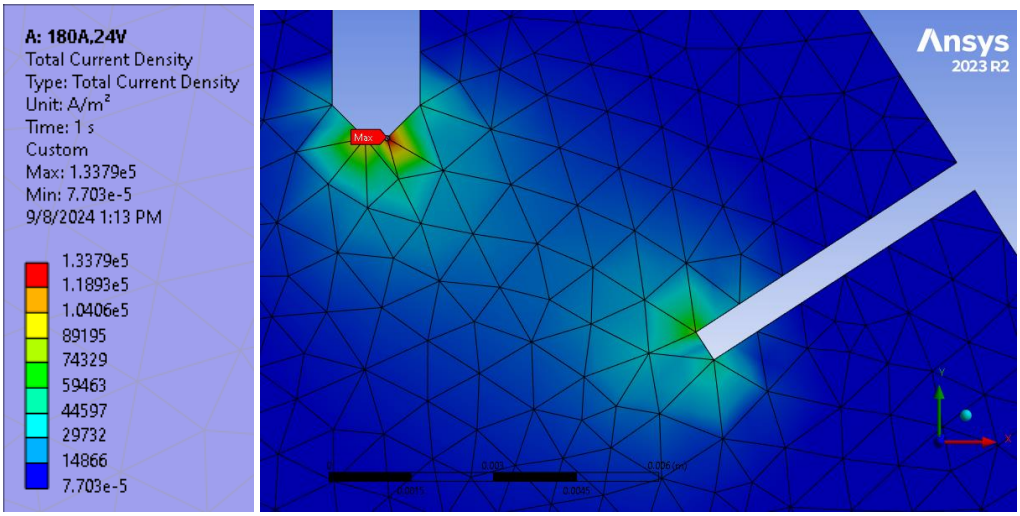

Figure 5. Current density set 1

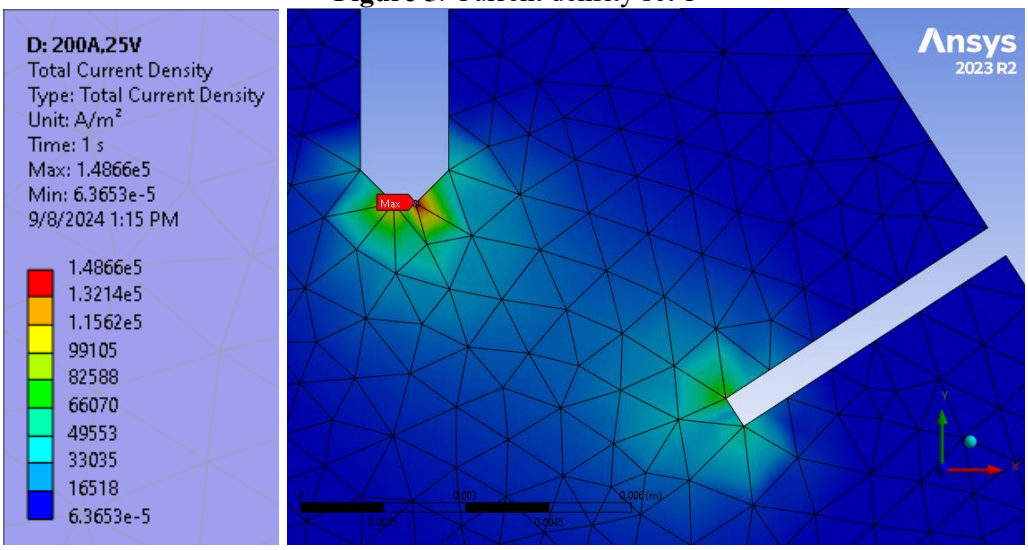

Figure 6. Current density set 2

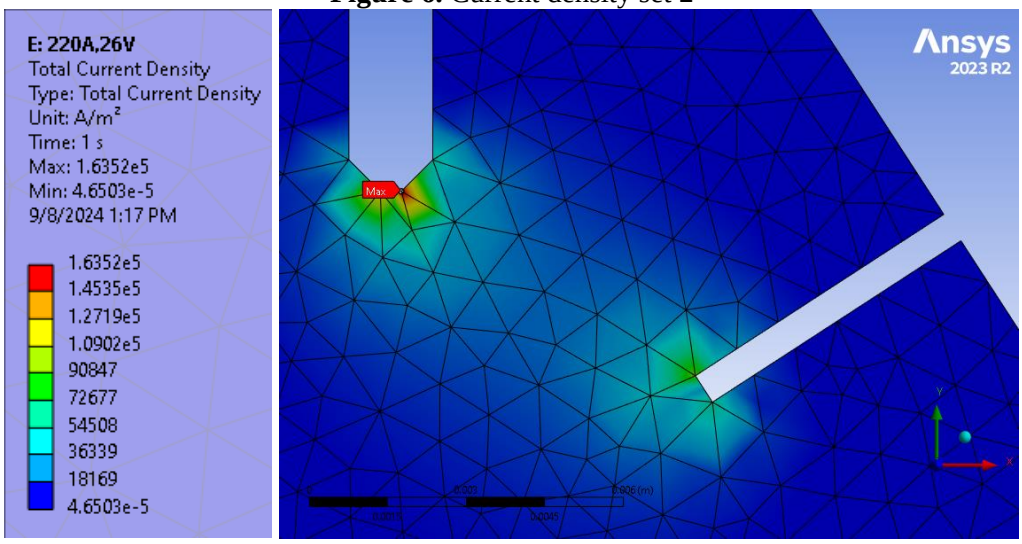

Figure 7. Current density set 3

The red zone in Figure 8 indicates regions of maximum heat flux at the TIG and MIG tips during the hybrid welding process. The heat flux value is important, particularly in the welding process that involves in heat transfer process. Heat flux is defined by the amount of heat transferred per unit area per unit of time to a surface or from a surface. Accurate control of heat flux is essential for predicting and controlling the thermal stresses and distortions, which are critical factors in the integrity and performance of the welded structure. The resulting value of heat flux is used to optimize the welding parameters for achieving the desired thermal distribution, which influences the microstructure and mechanical properties of the welded joint. It ensures that the energy from the welding processes is efficiently utilized, leading to improved weld quality and reduced defects.

Referring to Table 4, after the simulation of 3 sets of parameters, it was found that the heat flux value at each MIG tip and TIG tip did not change even though there have been changes to higher voltages and the current value. The interaction of two welding tips is visualized in Figure 8 which is only from the result from set 1 (180A and 24V), because after the other set was executed, the value of heat flux was the same. The recorded heat flux values were 1.66 MW/m² for the TIG tip and 0.95 MW/m² for the MIG tip. However, the value still needs to be used in the next analysis. In this case, the heat flux value is taken from the surface of the MIG and TIG tips. After that, the simulation continued to the Fluent analysis by inserting the value of heat flux into the boundary condition of the torches walls. The simulation results were validated against experimental data obtained from previous studies which is the Cui et al. research paper.

Table 4. Heat flux result for 3 sets

THERMAL-ELECTRIC	Result
HEAT FLUX	TIG TIP: 1,663,300 W/m^2 MIG TIP: 950,390 W/m^2

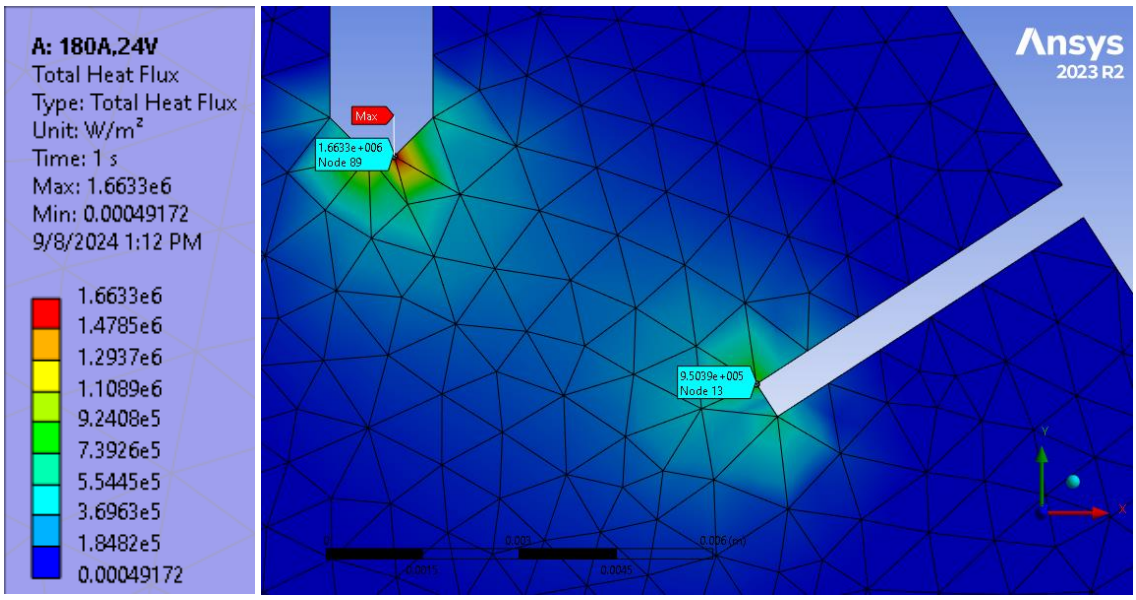

Figure 8. Heat flux for 3 sets

3.2. Ansys Fluent analysis

The results from Fluent analysis are shown in Table 5. Regarding Figure 9, the red zone indicates the maximum temperature distribution which recorded approximately 3409.77°C during the welding process. This high temperature is approximated at the areas close to the welding arc, where the energy input from both TIG and MIG processes is concentrated. Red zones represent the highest temperature regions, while blue zones indicate cooler areas. At the red zone, the maximum heat load is experienced by the material, which is essential to understanding the effectiveness of the welding process. The shape of this distribution is due to the nature of heat transfer during welding. Heat is most intense at the source (the welding arc) and gradually dissipates as it moves away from it. This gradient significantly influences the fusion and solidification processes, thereby directly impacting weld quality. The heat flux value set in the boundary condition directly influences the extent of the red zone. Higher heat flux results in a larger and more intense red zone, indicating higher temperatures. Fundamentally, the heat flux determines how much energy is input into the material being welded. The intense heat in this area is necessary to achieve proper penetration and fusion of the materials being welded. However, this also presents risks such as overheating or distortions if not managed properly. Therefore, controlling the extent of the red zone through an accurate parameter is essential to optimize the welding quality.

Table 5. Temperature and velocity distribution result

FLUENT	Heat flux	
TEMPERATURE AND VELOCITY DISTRIBUTION	TIG TIP: 1,663,300 W/m^2, MIG TIP: 950,390 W/m^2	
	Maximum temperature: 3409.77°C	Maximum velocity: 7.73 m/s

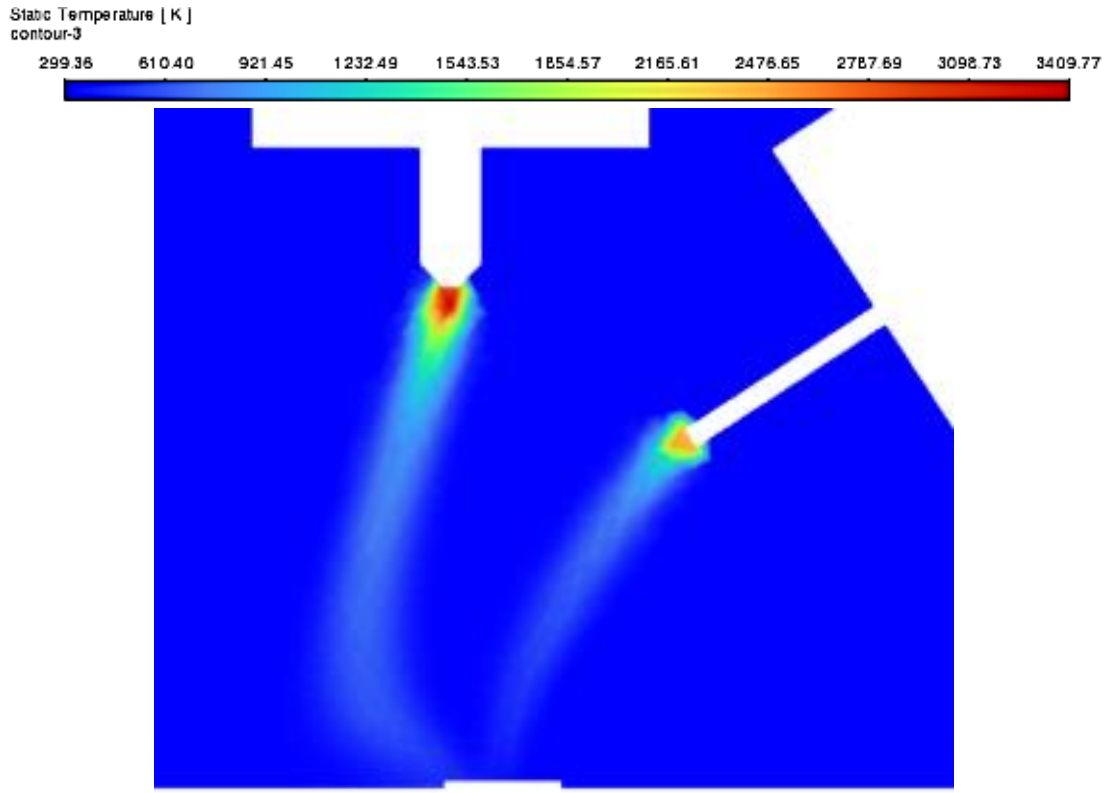

Figure 9. Temperature distribution

Figure 10 illustrates the velocity distribution represents the flow of plasma or gas during welding. The maximum velocities can reach approximately 7.73 m/s. The red zone indicates the highest velocity, while the blue zones represent lower velocities. This high velocity at the red zone is significant because it affects how heat is distributed across the weld area. High velocity in this region is likely due to the dynamic effects of the shielding gas flow and the movement of the molten pool during the welding process. Regions with higher velocities experience more efficient heat exchange. Consequently, affects how heat is distributed across the weld area. Also, the red area indicates the area, where the molten material moves faster, which can significantly affect the cooling rate. The cooling rate directly influences the microstructure of the weld. Higher speeds can result in faster cooling rates, which can affect microstructure formation in the weld and lead to high strength and toughness of the welded metal.

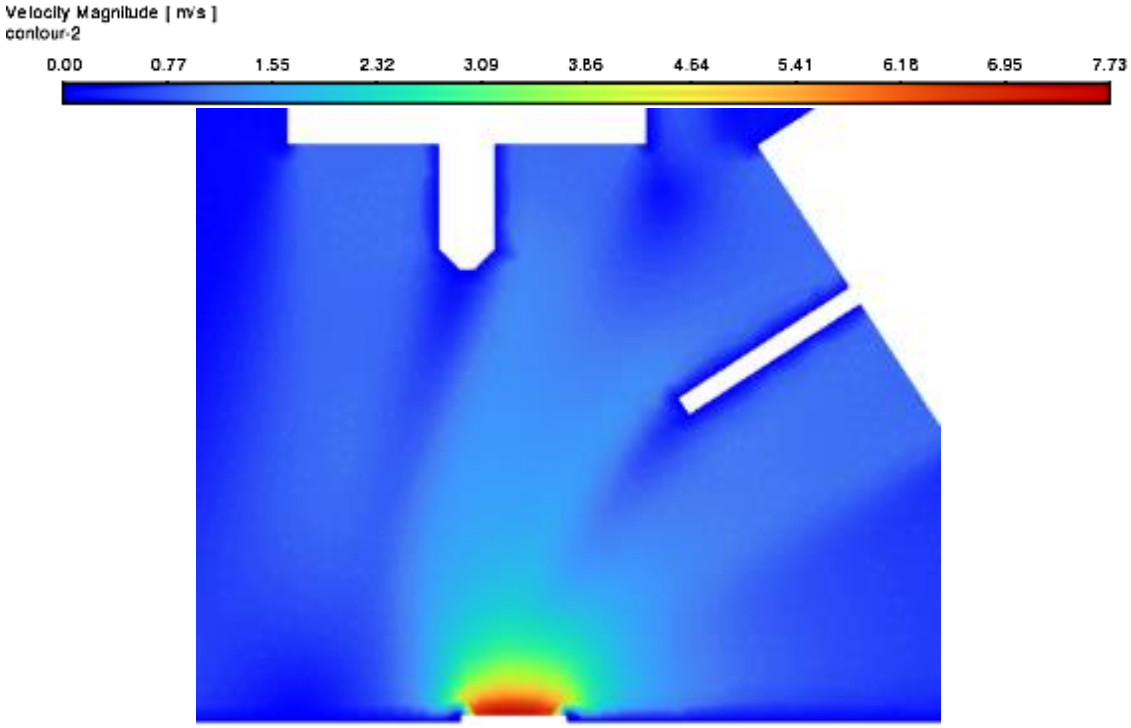

Figure 10. Velocity distribution

4. Result Validation

For heat flux at the TIG tip, the previous study with the same material used, and the same heat input (current ~200A), reports a typical range of heat flux values around 1.5×10^6 W/m^2 to 1.8×10^6 W/m^2 for TIG/MIG hybrid welding processes. Besides, the heat flux values for the MIG tip in hybrid welding processes are reported to be around 9.0×10^5 W/m^2 to 1.2×10^6 W/m^2. The variation calculation was calculated using the formula below;

$$\frac{|\,Experimental - simulation|}{|Experimental|} \times 100 = variation\ error \tag{13}$$

Table 6 shows the validated experimental values from Cui et al [7] confirming that the heat flux in TIG/MIG hybrid welding processes falls within a specific range. The simulation results show good agreement with the experimental values, with variation errors of 2.16% for the TIG tip and 4.96% for the MIG tip, indicating the reliability of the simulation model. This validation supports the accuracy of this simulation results and provides a solid foundation for this study.

Table 6. Validation result

Welding Tip	Information	Variation Error
Heat flux for TIG	Experimental value: 1.7 MW/m^2 Simulation result: 1.67 MW/m^2	2.16%
Heat flux for MIG	Experimental value: 1.0 MW/m^2 Simulation result: 0.95 MW/m^2	4.96%

5. Conclusion

The study successfully demonstrated that the use of Computational Fluid Dynamics (CFD) simulations can effectively model and analyze the TIG/MIG hybrid welding process. Key findings include the significant impact of varying current and voltage on current density distribution, particularly near the TIG tip, while heat flux remained relatively unaffected. The heat flux values recorded were 1.66 MW/m² at the TIG tip and 0.95 MW/m² at the MIG tip, indicating that factors other than current and voltage influence heat distribution. The numerical simulation results demonstrated high accuracy, with variation errors of 2.16% for the TIG tip and 4.96% for the MIG tip compared to experimental values, confirming the reliability of the CFD model used in this study. Additionally, the maximum temperature recorded during the simulation was 3409.77°C, and the maximum velocity of the shielding gas or movement of the molten pool was 7.73 m/s, providing essential information for understanding the thermal environment and cooling rates in hybrid welding. The simulation results were validated against experimental data from Cui et al, confirming that the heat flux values for TIG and MIG tips are within the expected ranges. This validation underscores the robustness of the simulation approach and its applicability for further research such as conducting experimental studies to further validate simulation results of the effects of current density toward the penetration weld strength.

6. Acknowledgments

The authors would like to acknowledge the support from the Ministry of Higher Education Malaysia and Research Management Centre (RMC), Universiti Malaysia Perlis (UniMAP) for awarding the research grant under Collaborative Research Grant: project number: 9023-00025 undertaking this project.

7. References

[1] C. S. Abima, S. A. Akinlabi, N. Madushele, and E. T. Akinlabi, “Comparative study between TIG-MIG Hybrid, TIG and MIG welding of 1008 steel joints for enhanced structural integrity,” *Sci. African*, vol. 17, p. e01329, 2022, doi: 10.1016/j.sciaf.2022.e01329.

[2] Y. Zhao and H. Chung, “Numerical simulation of the transition of metal transfer from globular to spray mode in gas metal arc welding using phase field method,” *J. Mater. Process. Technol.*, vol. 251, pp. 251–261, Jan. 2018, doi: 10.1016/j.jmatprotec.2017.08.036.

[3] T. Kik, “Heat Source Models in Numerical Simulations of Laser Welding,” *Materials (Basel).*, vol. 13, no. 11, p. 2653, Jun. 2020, doi: 10.3390/ma13112653.

[4] Y. Sangwan, S. Singhal, K. Narayan, and B. Sumit, “A Review on TIG / MIG Welding Process : Recent Advances and Future Directions,” vol. 11, no. 10, pp. 57–62, 2023.

[5] R. Zong, J. Chen, and C. Wu, “A comparison of TIG-MIG hybrid welding with conventional MIG welding in the behaviors of arc, droplet and weld pool,” *J. Mater. Process. Technol.*, vol. 270, pp. 345–355, Aug. 2019, doi: 10.1016/j.jmatprotec.2019.03.003.

[6] W. Gou and L. Wang, “Effects of welding currents on microstructure and properties of 5052 aluminum alloy TIG welded joint,” *IOP Conf. Ser. Mater. Sci. Eng.*, vol. 772, no. 1, 2020, doi: 10.1088/1757-899X/772/1/012011.

[7] X. Cui, J. Chen, C. Xia, X. Han, H. Su, and C. Wu, “The mechanism study of TIG-MIG hybrid welding process based on simulation,” *Vacuum*, vol. 215, p. 112341, Sep. 2023, doi: 10.1016/j.vacuum.2023.112341.